04

System of the resonant magnetic fields genereation in the T-10 tokamak

© E.A. Shestakov,[1] P.V. Savrukhin[1,2]

[1] National Research Center, „Kurchatov Institute“,
123182 Moscow, Russia
[2] National Research University „Moscow Power Engineering Institute“,
111250 Moscow, Russia
e-mail: shestakov_ea@nrcki.ru

Received May 23, 2024
Revised October 14, 2024
Accepted October 21, 2024

A description is given of a system for generating resonant magnetic fields in the T-10 tokamak for controlling magnetohydrodynamic (MHD) plasma perturbations and correcting error magnetic fields. The system is based on 8 multipole windings located on the outside of the torus to create resonant magnetic fields with poloidal and toroidal harmonics $m = 1-4$, $n = 1$. The power supply of the T-10 windings is provided on the basis of controlled thyristor converters. The control system is based on Siemens S7 controllers and combines programmable logic controllers, diagnostic information input units, galvanic insulators and control system parameter sensors.

Keywords: tokamak, resonant magnetic fields, magnetohydrodynamic plasma perturbations, multipole windings, programmable logic controllers.

DOI: 10.61011/TP.2025.01.60505.188-24

Introduction

The retention of high-temperature plasma in tokamak installations is limited by the development of various magnetohydrodynamic (MHD) instabilities leading to saturation β_t (the ratio of plasma pressure to the pressure of the retaining magnetic field), and in some cases to plasma disruption [1–3]. Generally, disruptions at high β_t are associated with ideal helical modes developing near the boundary of the plasma cord. Helical modes can be stabilied by external magnetic fields resonant with plasma disturbances [1,4–6]. The amplitude and phase of the currents in the external windings are determined in this case by a feedback system based on measurements of electromagnetic plasma disturbances [1,3,7].

The development of internal MHD perturbations (tearing modes) is also possible in a plasma with finite conductivity [2,8], leading to the formation of magnetic islands near resonant surfaces inside the plasma. The growth of magnetic islands can stop the rotation of MHD perturbations and cause the plasma disruption at a lower level of β_t than the limit imposed by external modes. The stability of the tearing modes depends on the plasma current profile and boundary conditions in case of low values of β_t. The development of tearing modes can be delayed and in some cases prevented by changing the boundary conditions using the external resonant magnetic fields [9–14].

One of the most important tasks of the external resonance field generation system is the correction of scattered magnetic fields of the tokamak, which are caused by the inaccuracy of the assembly of the magnetic system, the heterogeneous arrangement of current leads and diagnostic systems, and additional plasma heating [1,15–17]. Scattered magnetic fields can cause a slowdown of the rotation and stopping of magnetic islands, and a subsequent increase of MHD disturbances and plasma disruption. The compensation of scattered fields is especially important in case of operation in low-density modes at the initial stage of discharge and during additional heating using neutral particle injection [18,19].

This paper considers a system for generating external resonant magnetic fields installed on tokamak T-10. Section 1 describes multipole (saddle) and stochastic windings on tokamak T-10. The control and data logging system, as well as the winding power supply system, are discussed in section 2.

1. Multipole and stochastic windings on tokamak T-10

External resonant magnetic fields are generated by a system of multipole (saddle) windings on tokamak T-10 (Fig. 1). The windings are located outside the vacuum chamber on the outside of the winding blocks of the toroidal field evenly along the toroidal bypass of the tokamak. The main parameters of the windings are listed in the following table. The dimensions and location of the windings are selected taking into account the diagnostic pipes of tokamak T-10. The parameters of the saddle windings were also determined so that maximum current modes can be used in the conductors with the specified parameters of the thyristor converters VDU-1250 (current $I_{SC} = 1250$ A, voltage $V_{SC} = 55$ V).

Rectangular multi-turn saddle windings with rounded corner sections with a base width of $L_{SC} \approx 2$ m and a height of $H_{SC} \approx 1.5$ m are provided to ensure the maximum

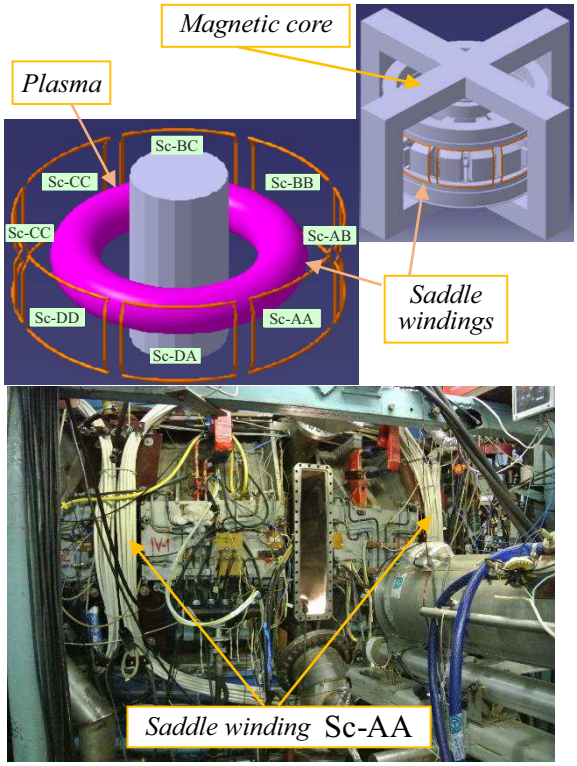

Figure 1. *a* — layout view of eight external saddle windings (SC) on tokamak T-10; *b* — photo of the location of the SC-AA winding (white cables).

Parameters of external resonant windings on tokamak T-10

Winding type	Saddle windings	Stochastic windings
Number of windings	8	16
Number of turns in the winding	11	20
Dimension	Width $L_{SC} \approx 2$ m Height $H_{SC} \approx 1.5$ m	Diameter of turns $D \approx 28.5$ cm
Inductance	490 μH	22 μH
Resistance	11 mΩ	7 mΩ

amplitude of the magnetic fields (Fig. 1). Each winding consists of $N_{turn} = 11$ turns of PV-3 1x120 V cable with PVC insulation (cross-sectional area of the current conducting conductor is 120 mm^2).

The polarity of the currents in the windings is set before the start of the experiments and can be changed in the intervals between the pulses. Saddle windings in opposite octants are connected in antiphase in the standard experimental setup to generate the maximum amplitude of toroidal harmonics $n = 1$. Four pairs of windings are switched on independently during the tokamak pulse.

The amplitude of the magnetic fields generated by the saddle windings was calculated using the finite difference element method of the equations of electrostatics and magnetostatics, taking into account the design features of tokamak T-10 [20] based on the Bio–Savart–Laplace equation, taking into account the imposed boundary conditions. The results of the calculation of the magnetic fields generated by the saddle windings on tokamak T-10 are shown in Fig. 2. The saddle windings were represented in the form of rectangular frames located in the angular and radial positions specified based on the experiment. The amplitude of the toroidal and poloidal harmonics was determined by decomposing of the calculated magnetic fields on the resonant magnetic surface $q = 2$ into a Fourier series (Fig. 2, *d*). It should be noted that the presence of the magnetic core of tokamak T-10 distorts the magnetic field created by the windings and slightly enhances it compared to calculations without the magnetic core.

The representation of resonant windings in the calculation of magnetic fields in the form of linear conductors is a simplified model. Rectangular coils with rounded corners are used in experiments on tokamak T-10 (Fig. 1). The change of the magnetic field with relatively small deviations of rectangular windings with rounded corners from rectangular frames in tokamak T-10 does not exceed 2% and does not significantly distort the amplitudes of the lower harmonics $m < 3$.

The amplitude of resonant magnetic fields was measured in experiments on tokamak T-10 using a system of 24 magnetic probes. The magnetic probes were positioned uniformly along the poloidal circumference of the torus in a thin-walled metal tube located on the wall of the vacuum chamber (small radius $r_p = 0.4$ m). The amplitude of the poloidal component of the external resonant magnetic fields when the external fields are turned on is shown in Fig. 3. The magnetic probes have the same orientation along the tube axis. This leads to the fact that, for example, the upper and lower probes (see MM7 and MM19 in Fig. 3) have the opposite orientation in the coordinate system associated with tokamak T-10. The maximum amplitude of the external poloidal magnetic field at the boundary of the vacuum chamber ($R = 1.5$ m, $a_p = 0.4$ m, $\vartheta = \pm\pi/2$) at currents in the saddle windings $I_{SC} = 1250$ A reaches $B_p = 6-7$ mT, which turns out to be close to the calculated values.

The speed of the external resonant fields depends on the rate of increase of currents in the saddle windings and on the time of penetration of magnetic fields inside the vacuum chamber of the tokamak. The oscillating external magnetic fields inside the vacuum chamber will be significantly weakened because the windings are located outside the vacuum chamber of the tokamak and are shielded by conductive structures, including, first of all, a conductive copper casing (with a wall thickness of 5 cm). Shielding structures also delay the penetration of external fields into the vacuum chamber when the currents in the saddle windings are switched on. This limits the possibility of using external windings to generate rapidly alternating

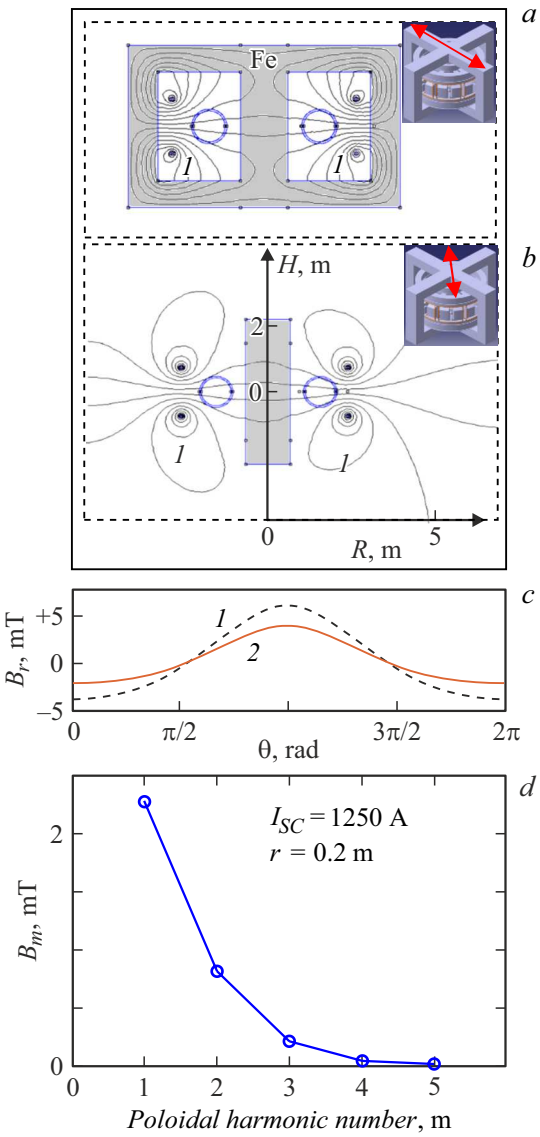

Figure 2. Results of calculation of stationary magnetic fields generated by two saddle windings (*1*) located in opposite octants of tokamak T-10 (current in windings is $I_{SC} = 1250$ A) in sections under the core of the magnetic circuit (*a*) and in intermediate sections (*b*). The location of T-10 magnetic core section is shown (gray rectangle — Fe) and a vacuum chamber with a casing (*3*); *c* — the amplitude of the radial magnetic field on a magnetic surface with a small radius $r = 20$ cm ($R_0 = 1.5$ m) taking into account (*1*) and excluding the magnetic core (*2*), θ — poloidal angle; *d* — amplitude of the poloidal harmonics of the magnetic field, created by eight windings included to create a spatial structure with a toroidal harmonic $n = 1$, calculated on a magnetic surface with a small radius $r = 20$ cm ($R_0 = 1.5$ m).

magnetic disturbances. Calculations show that the time constant of the chamber of tokamak T-10 ($\tau_w = 3$ ms) is much longer than the characteristic current rise times in the windings, determined by inductance ($L_{SC} = 490\,\mu$H) and resistance ($R_{SC} = 11$ MΩ): $\tau_{SC} = L_{SC}/R_{SC} \approx 44\,\mu$s).

The rise time of magnetic fields inside the vacuum chamber is determined by the speed of thyristor converters in experiments on tokamak T-10. A typical time evolution of the signal of a magnetic probe located inside a vacuum chamber on the outside of the torus near the equatorial plane when the currents in the windings are switched on is shown in Fig. 3. The inclusion of currents in the windings ($t = 560$ ms) corresponds to an increase of the poloidal magnetic field with a characteristic rise time $dt \sim 35-40$ ms.

The relatively long rise time of the amplitude of the magnetic fields generated by the windings is determined by the design of VDU-1250 thyristor converter units operating based on the inverter converter circuit designed to maintain a stable output current with a rigid external characteristic.

„Stochastic“ windings were provided to generate external magnetic fields at the first stage of experiments on tokamak T-10. The „stochastic“ windings were arranged in pairs in eight sections around the torus, symmetrically relative to the equatorial plane of the torus (Fig. 4). Each winding consists of $N_{turn} = 20$ turns of a copper conductor (cross section 12×12 mm with an internal water cooling channel $d \sim 5$ mm) wound in the form of a winding with a diameter of $D \sim 28.5$ cm.

Calculations show that at maximum currents in such windings (current density up to 100 A/mm^2 in a pulse up to 100 ms), the radial magnetic field from one winding in the equatorial plane on a surface with radius $R = 1.75$ m is 1.2 mT. Switching on the windings in pairs in antiphase (the polarity of the connection can be changed to create magnetic fields of various configurations) should create alternating „stochastic“ magnetic fields in the peripheral regions of the plasma on the outer edge of the torus (toroidal and poloidal harmonics up to $n = 7$, $m = 7$). Unfortunately, VDU-1250 thyristor converters used in experiments on T-10 provide up to 1250,A (10,A/mm^2) currents in stochastic windings, which is an order of magnitude lower than the calculated values. The inclusion of „stochastic“ windings did not lead to any noticeable effect on plasma parameters in tokamak T-10 under these conditions.

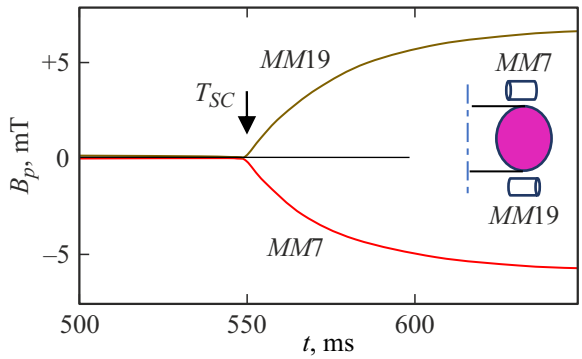

Figure 3. Temporal evolution of the amplitude of the external magnetic field when currents are switched on in the saddle windings ($T_{SC} = 550$ ms, current in the windings $I_{SC} = 1250$ A), measured using poloidal magnetic probes located at the boundary of the vacuum chamber above and below relative to the equatorial plane of the torus (MM7 — $\vartheta \approx 90°$, MM19 — $\vartheta \approx 270°$).

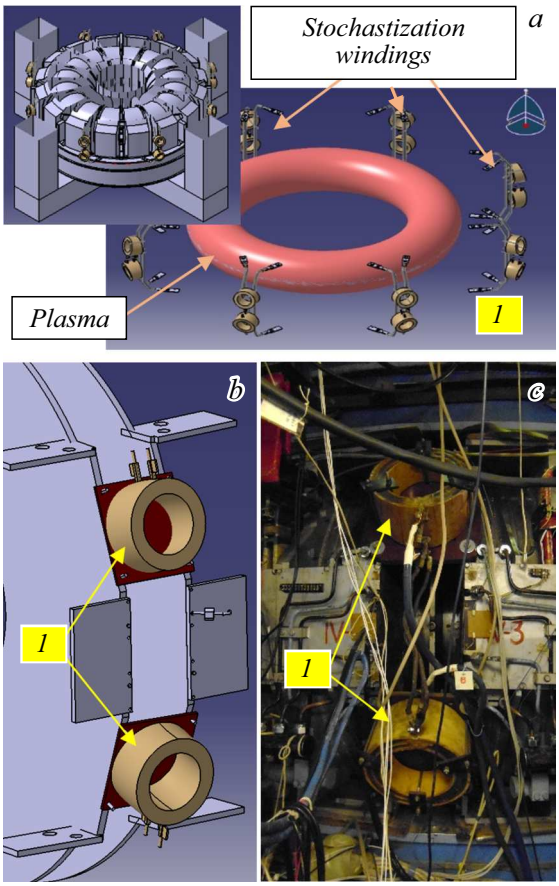

Figure 4. Schematic representation of external „stochastic“ windings (*1*) (*a*, *b*) and *c* — photo of two „stochastic“ windings on tokamak T-10.

2. Power supply and control system for resonant magnetic field windings on tokamak T-10

The winding power supply system for generating resonant magnetic fields on the tokamak T-10 is based on VDU-1250 thyristor converters (Fig. 5, 6) with control based on Siemens S7 controllers [21], combining programmable logic controllers, galvanic insulator blocks and control system parameter sensors. Power supplies generate current pulses in the saddle windings based on programs set by the operator before starting experiments.

VDU-1250 controlled thyristor converters are located in the compartment under T-10 installation. The power supplies are based on controlled three-phase thyristor rectifiers and supply a rated output current of $I = 1250$ A with a voltage of $V = 55$ V. A short-term increase of current to 1900 A is also possible. The maximum output voltage with a connected load is $V = 44$ V in this case. VDU-1250 converters have a remote control capability, which ensures turning the power supply on and off at specified times and allows for output voltage adjustment. VDU-1250 control units also allow measuring the basic parameters of an electrical circuit (output voltage, current, and a logic AC sensor).

Four power sources with a total power of up to 300 kW are used in experiments on tokamak T-10. The external windings are connected to the power supply in pairs, the two windings opposite relative to the main axis of the tokamak are connected in series so that the magnetic field generated by them is directed in one direction. The total resistance of the circuit, taking into account the supply cables with this type of connection, is equal to $R_{SC\_Tot} = 30$ mΩ, and the maximum possible current in the circuit can reach $I_{SC\_max} = 1260$ A, which corresponds to the rated current of the converter.

The rectifier can operate in the overload mode since the windings are expected to operate in the pulse mode. Two windings can be connected in parallel to each power source to increase the amplitude of the magnetic fields. The maximum current through the power supply can reach 2500 A in this case with a current pulse duration of no more than 2 s.

Tokamak T-10 power supply control system is based on Siemens S7-417 programmable logic controllers (PLC). A

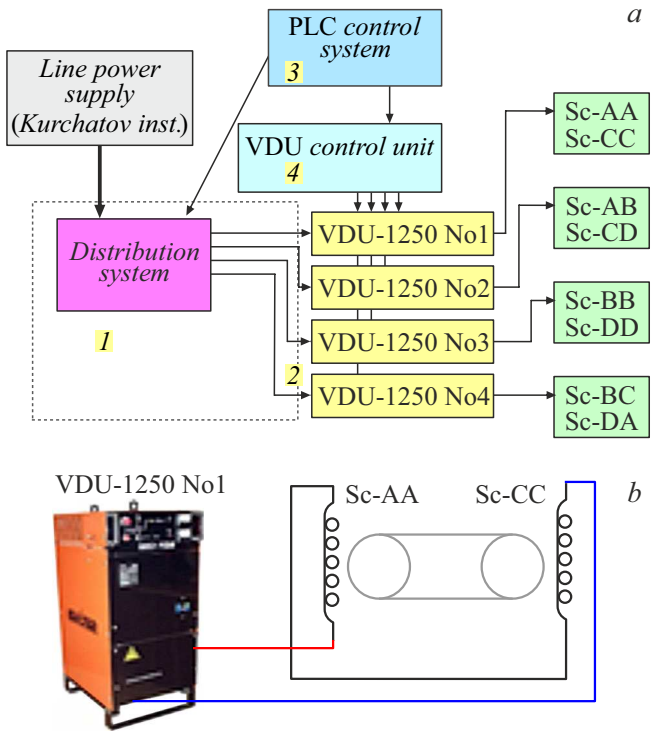

Figure 5. *a* — schematic representation of the power supply system for saddle windings on T-10 installation. The dotted line indicates the power supply connection module (*1*) with an interlocking and emergency shutdown system. The operating mode of VDU-1250 thyristor converters (*2*) is set by the control system based on S7-417 controller (*3*) remotely from tokamak T-10 control room and locally from VDU-1250 control panel(*4*); *b* — diagram of the standard connection of saddle windings to VDU-1250 thyristor converters. The windings in opposite octants are connected in antiphase (see Sc-AA and Sc-CC in Fig. 1).

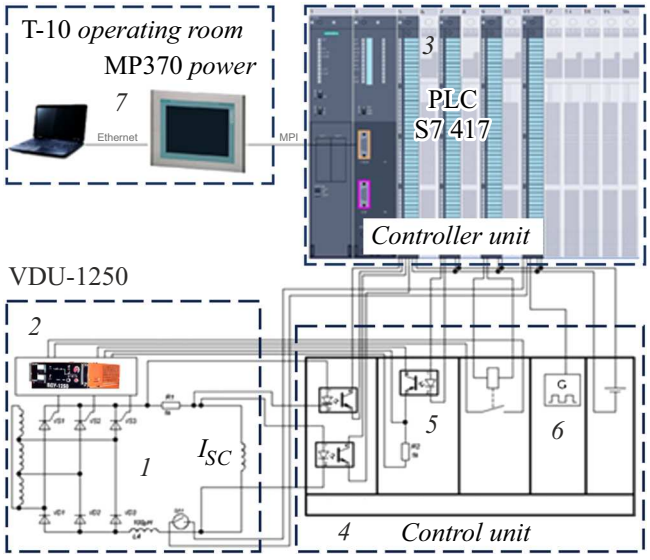

Figure 6. Schematic diagram of power supply control of a resonant magnetic field generation system. The currents in the windings (I_{SC}) are set by the control signals of VDU-1250 control board (*1*) based on local control signals from VDU-1250 control panel (*2*) or remotely based on the commands of S7-417 controller(*3*). The control unit (*4*) matches the input and output signals of the controller unit and VDU-1250 based on optical isolation amplifier modules (*5*) and an external clock generator (*6*). S7-417 controller is controlled remotely using MP370 mobile operator panel (*7*) located in the control rack in Tokamak T-10 control room.

schematic diagram of the power supply control system is shown in Fig. 6. The control system ensures the activation of resonant magnetic fields in stationary and alternating modes (frequency up to 10 Hz) at the time points set by the operator independently for four pairs of saddle windings. Both remote control from T-10 control room and direct control is possible using the control panel modules of VDU-1250 converters. The system is monitored by recording resonant magnetic fields with standard magnetic probes of T-10 installation and loop probes provided to measure quasi-stationary radial magnetic fields. The control system based on the S7-417 controller on tokamak T-10 sets the program for switching on the voltage by power sources in accordance with the program and measuring the main control parameters, including output voltage and current in windings.

S7-417 controller, provided on tokamak T-10, is a modular control system that includes a crate (UR1 mounting rack), a controller unit and a set of I/O modules interconnected by a common power and data bus. The power is supplied to the control system by PS 407 stabilized power supply unit ((5 V)/(20 A)).

Optical decoupling in the S7 modules is provided at the stage of digital data transfer between the modules and the internal data bus of the controller. Special isolation circuits are provided to prevent galvanic coupling of power supplies and the control system. The output voltage and voltage signals on the current measuring shunt, which determines the output current, are supplied to the KFKI optical isolation amplifier module with a signal conversion frequency of 100 kHz. The module has a gain $K_{\text{gain}} \sim 5$ and operates in both positive and negative input signal ranges. The converted signals are supplied from the output of this module to the analog to digital converter (ADC) module of the Siemens SM 431 controller. The current sensor is a sealed contact (reed switch) that closes when a magnetic field is applied and is located near one of the output busbars. The sensor parameters and its location are designed for closing when the current in the bus exceeds 100 A.. This sensor does not require additional galvanic isolation, its signal is supplied to the discrete signal input module SM 421.

The operating mode of VDU-1250 thyristor converters is set using an integrated control board that supplies pulses to the thyristor gates in accordance with control signals and current and voltage feedback signals. The power supply is switched on and off by closing the control contacts using a relay (the signal from one contact group controls the power supply, the signal from the second contact group is transmitted to the PLC). The output voltage is changed by changing the input voltage of the control board in the range $V_{\text{out}} \sim 0-15$ V. A circuit solution based on 4N25 optocoupler was used to implement galvanic isolation and matching with SM 432 DAC module.

The synchronous pulse signal is used for peripheral modules data collection and recording in the PLC. This signal can be supplied both by an internal timer or an external generator set by synchronous pulses of tokamak T-10. S7-417 controllers are provided with built-in timers with a response period of at least 10 ms, however, peripheral modules allow data collection with a higher frequency, therefore, an additional external highly stable oscillator with an adjustable frequency in the range of 100 Hz–2 kHz is used for synchronization. Data are recorded in the internal memory of the PLC. The service variables are also stored there.

The control system is controlled using MP370 mobile operator panel located in the control rack in the control room of tokamak T-10.

MP370 panel data and PLC data are synchronized using the PROFIBUS interface. PROFIBUS is an industrial data transmission standard and operates using the master-slave principle. The data transfer rate in the network is 12 Mbit/s, the length of the transmission line without repeaters on T-10 installation $L \sim 100$ m. The operator uses the panel to determine the operating mode of each of the four power sources before the next plasma discharge of tokamak T-10, determining, in particular, the number of power-on cycles, the start-up time, the duration of pulses and pauses of operation. After confirming the set operating modes and previewing the corresponding waveforms, the control data is recorded in arrays of control parameters. After the arrival of the trigger pulse, the PLC outputs control signals in accordance with the data in these arrays. The system can

be started either from the starting signal of tokamak T-10, or manually at the operator's command.

After the discharge is completed and the signals from the peripheral modules are recorded in the data blocks, the PLC transmits all data arrays to the operator panel for further analysis. Writing to general Tokamak T-10 database of a PC is carried out over an Ethernet network using script commands with the possibility of subsequent processing and archiving.

An emergency shutdown unit is provided to quickly turn off the power supply to the frame windings in case of an emergency. The unit initiates the disconnection of the contactor of the power supply module by the operator's command from T-10 control room based on the readings of current sensors and in case of unauthorized access to VDU-1250 compartment.

3. Results of experiments using saddle windings on tokamak T-10

The effect of magnetic fields generated by saddle windings on the MHD stability of plasma is most clearly manifested in experiments on tokamak T-10 in modes with a stability margin at the boundary of the plasma cord $q_a \approx 3$ (plasma current $I_p = 290$ kA, longitudinal magnetic field $B_t = 2.4$ T). The development of MHD perturbations

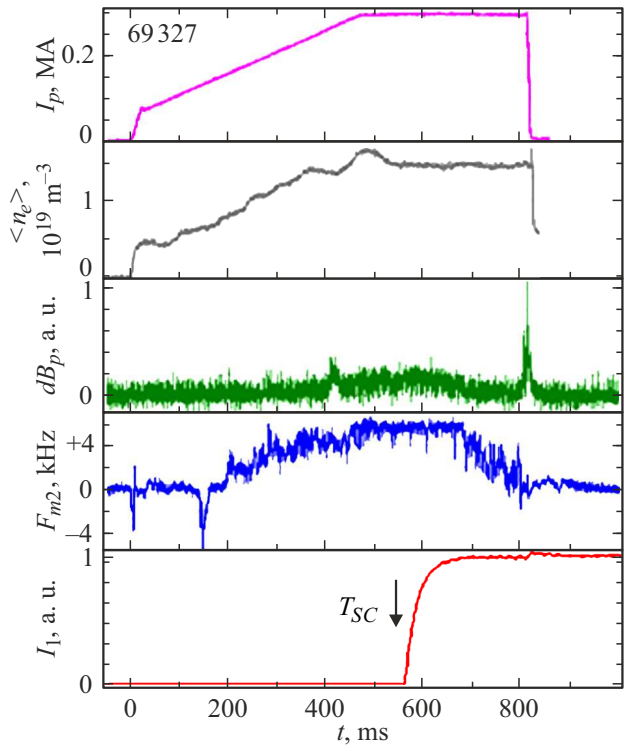

Figure 7. Temporal evolution of plasma parameters in tokamak T-10 when resonant magnetic fields are turned on: Ip — plasma current; $\langle n_e \rangle$ — electron density; dBp — amplitude of disturbances of poloidal magnetic fields $m = 2$, $n = 1$; F_{m2} — rotation frequency of the mode $m = 2$, $n = 1$; I_1 — current in saddle windings.

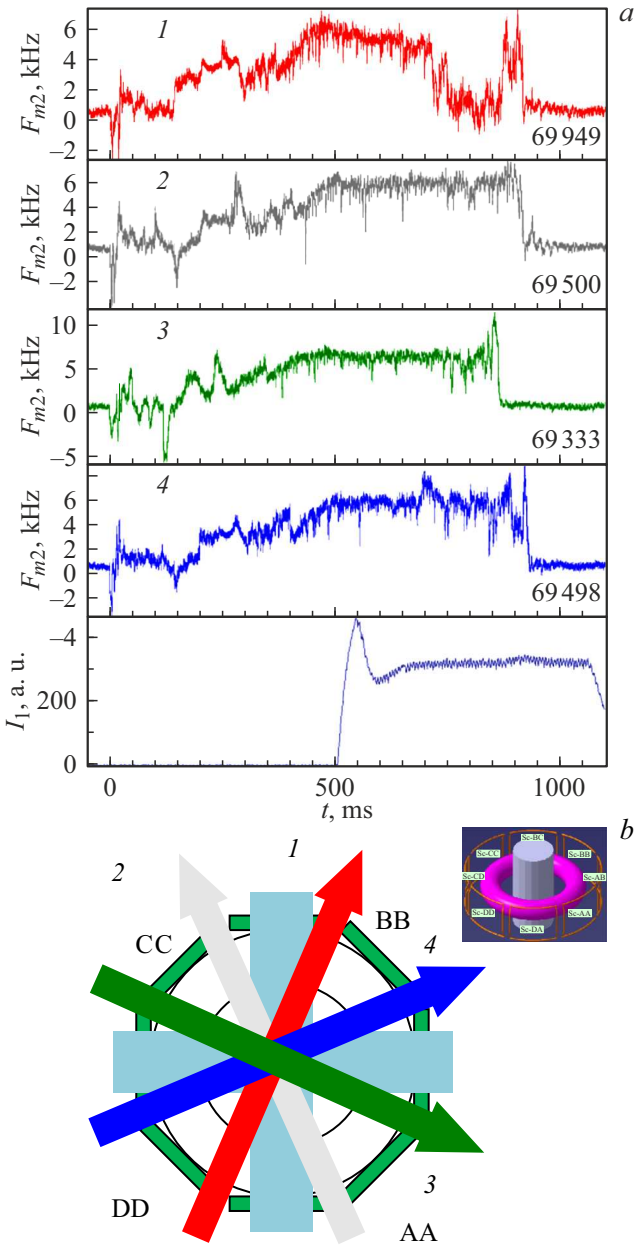

Figure 8. a — temporal evolution of the rotation frequency of MHD perturbations $m = 2$ (F_{m2}) in tokamak T-10 at different directions of the external magnetic field. The current in the saddle windings is also shown (I_1); b — schematic representation of the plasma cord and the system of saddle windings in tokamak T-10. The arrows show the direction of the resulting external magnetic fields generated by the saddle windings in a series of successive pulses of tokamak T-10. The numbers near the waveforms correspond to the numbers near the direction arrows of the external magnetic field.

with poloidal and toroidal numbers $m = 2$, $n = 1$, rotating at a frequency of $f \sim 4-6$ kHz is observed under these conditions at the stationary stage of the discharge ($t = 300-600$ ms in Fig. 7). The rotation frequency of the MHD perturbations slows down when external

resonant magnetic fields are turned on in this discharge mode of T-10 ($t > 670$ ms in Fig. 7). The characteristic deceleration time of MHD perturbations $\Delta f/\Delta t \sim 50$ kHz/s corresponds to the predictions of model calculations [19,20]. It should be noted that the MHD perturbation deceleration is nonmonotonic ($t \sim 680-800$ ms in Fig. 7): periodic sharp increases and decreases of rotational speed are observed with a general tendency towards a decrease of the rotational speed, which is generally consistent with the models of destabilization of the tearing modes [5,8,12]. After a complete stop of rotation („locking“ mode), a sharp increase of the amplitude of MHD disturbances is observed, followed by a disruption of the plasma discharge ($t > 815$ ms in Fig. 7).

Experiments on tokamak T-10 have shown that the effect of external fields on the MHD stability of the plasma significantly depends on the spatial orientation of the external resonant magnetic field. This effect manifests itself most clearly when analyzing the rotational velocities of MHD perturbations. The temporal evolution of the rotation frequency of the MHD perturbations $m = 2$ in tokamak T-10 in different directions of the external magnetic field is shown in Fig. 8. Deceleration of rotation and the effect of complete shutdown („locking“) of MHD disturbances (at specified reduced currents in the saddle windings, $I_{SC} = 640$ A) is observed only in case of one selected direction of external magnetic fields (1 in Fig. 8).

The direction of the magnetic field, which has a noticeable effect on the rotation frequency of magnetic disturbances, has a narrow spatial distribution and corresponds to the direction of the resulting magnetic field between the saddle windings Sc-BB and Sc-BC. This direction, apparently, coincides with the direction of the scattered magnetic field of tokamak T-10. The thresholds for stopping rotation of the MHD modes in a tokamak T-10 correspond to the amplitude of the scattered fields $B_{err} \approx 0.25$ mT. It should be noted that supply busbars are located near the Sc-BB windings to power the T-10 tokamak's poloidal and toroidal magnetic field winding system, and a shunt is located directly near the Sc-BB and Sc-BC windings to adjust the poloidal control magnetic fields.

Conclusion

A resonant magnetic field generation system has been developed and installed to control MHD plasma disturbances on tokamak T-10 which consists of eight saddle windings located symmetrically relative to the equatorial plane on the outside of the torus. The system allows generating magnetic fields with resonant harmonics $n = 1$, $m = 1-4$. The provided automated control system ensures the creation of quasi-stationary (duration up to 2 s) and pulsed (frequency up to 10 Hz) external resonant magnetic fields.

The analysis of the conducted experiments showed the following results: — the effect of slowing down the rotation of MHD modes is most pronounced in plasma modes when the resonant magnetic surface $q \approx 3$ is located near the plasma boundary;

— the deceleration rate of MHD perturbations increases non-linearly when the threshold value of the amplitude of external magnetic fields is exceeded;

— the braking effect of MHD perturbations depends on the spatial orientation of resonant magnetic fields. The effect of MHD perturbation deceleration is most pronounced when the direction of external resonant magnetic fields coincides with the direction of scattered fields of tokamak T-10.

T-10 resonant winding control system allows setting the currents in the windings according to a predefined program. Taking into account the nonlinear nature of the development of magnetic disturbances in the tokamak plasma, it is necessary to develop and use feedback system algorithms taking into account the dynamic parameters of the control system [9,12].

Standard magnetic probes are used as MHD perturbation sensors at T-10 installation [14,22]. Magnetic probes ensure the measurement of the amplitude and phase of magnetic disturbances, but they are also sensitive to changes of external magnetic fields. This makes it difficult to use them in a feedback control system. Diagnostics that are insensitive to alternating magnetic fields, such as X-ray and microwave radiation diagnostics, as well as radiation in the visible region can be used to reduce spurious signals in a feedback control system.

Resonant magnetic fields in tokamak T-10 are generated using multipole windings located outside the tokamak vacuum chamber. An analysis of previous experiments has shown that it is necessary to ensure the location of the windings inside the vacuum chamber in close proximity to the boundary of the plasma cord for an effective control of the plasma parameters. This arrangement will reduce the effect of shielding of resonant fields by in-chamber elements, including the protective plates of the first wall and limiters. The locations of the windings inside the vacuum chamber turn out to be especially important when considering the generation of variable resonant fields used to stabilize rotating MHD modes.

Acknowledgments

The authors would like to express their gratitude to N.A. Kirneva for stimulating discussions.

Funding

The study was supported by State Assignment regarding the Order of SRC„Kurchatovinstitute“.

Conflict of interest

The authors declare that they have no conflict of interest

References

[1] T.C. Hender, J.C. Wesley, J. Bialek, A. Bondeson, A.H. Boozer, R.J. Buttery, A. Garofalo, T.P. Goodman, R.S. Granetz, Y. Gribov, O. Gruber, M. Gryaznevich, G. Giruzzi, S. Günter, N. Hayashi, P. Helander, C.C. Hegna, D.F. Howel, D.A. Humphreys, G.T.A. Huysmans, A.W. Hyatt, A. Isayama, S.C. Jardin, Y. Kawano, A. Kellman, C. Kessel, H.R. Koslowski, R.J. La Haye, E. Lazzaro Y.Q. Liu, V. Lukash, J. Manickam, S. Medvedev, V. Mertens, S.V. Mirnov, Y. Nakamura, G. Navratil, M. Okabayashi, T. Ozeki, R. Paccagnella, G. Pautasso, F. Porcelli, V.D. Pustovitov, V. Riccardo1, M. Sato, O. Sauter, M.J. Schaffer, M. Shimada, P. Sonato, E.J. Strait, M. Sugihara, M. Takechi, A.D. Turnbull, E. Westerhof, D.G. Whyte, R. Yoshino, H. Zohm, and the ITPA MHD, Disruption and Magnetic Control Topical Group. Nucl. Fusion, **47**, S128 (2007). DOI: 10.1088/0029-5515/47/6/S03

[2] B.B. Kadomtsev. *Tokamak Plasma: A Complex Physical System, Plasma Physics Series* (IOP Publishing Ltd, 1992), p. 1–208.

[3] H. Zohm. *Magnetohydrodynamic stability of Tokamaks* (Weinheim: Wiley-VCH, 2015)

[4] M. Okabayashi, J. Bialek, M.S. Chance, M.S. Chu, E.D. Fredrickson, A.M. Garofalo, M. Gryaznevich, R.E. Hatcher, T.H. Jensen, L.C. Johnson, R.J. La Haye, E.A. Lazarus, M.A. Makowski, J. Manickam, G.A. Navratil, J.T. Scoville, E.J. Strait, A.D. Turnbull, M.L. Walker. DIII-D Team. Phys. Plasmas, **8**, 2071 (2001). DOI: 10.1063/1.1351823

[5] R. Fitzpatrick, A.Y. Aydemir. Nucl. Fusion, **36**, 11 (1996). DOI: 10.1088/0029-5515/36/1/I02

[6] T.E. Evans. Plasma Phys. Control. Fusion, **57**, 123001 (2015). DOI: 10.1088/0741-3335/57/12/123001

[7] T.H. Jensen, R. Fitzpatrick. Phys. Plasmas, **4**, 2997 (1997). DOI: 10.1063/1.872433

[8] P.H. Rutherford. Phys. Fluids, **16**, 1903 (1973). DOI: 10.1063/1.169423

[9] V.V. Arsenin, L.I. Artemenkov, N.V. Ivanov, A.M. Kakurin, L.I. Molotkov, A.N. Chudnovskii, N.N. Shvindt, Iu. Gvozdkov, M.Iu. Cherkashin. *Plasma Physics and Controlled Nuclear Fusion Research* (Innsbruck, 1978 (International Atomic Energy Agency, Vienna, 1979)), v. 1, p. 233.

[10] A.W. Morris, T.C. Hender, J. Hugill, P.S. Haynes, P.C. Johnson, B. Lloyd, D.C. Robinson, C. Silvester, S. Arshad, G.M. Fishpool. Phys. Rev. Lett., **64**, 1254 (1990). DOI: 10.1103/PhysRevLett.64.1254

[11] S.V. Konovalov, A.B. Mikhailovskii, E.A. Kovalishen, F.F. Kamenets, T. Ozeki, M.S. Shirokov, T. Takizuka, V.S. Tsypin. Dokl. Phys., **49**, 405 (2004). DOI: 10.1134/1.1784852

[12] P.V. Savrukhin. J. Computer and System Sciences Intern., **39** (3), 354 (2000).

[13] R. Fitzpatrick. Nucl. Fusion, **33**, 1049 (1993). DOI: 10.1088/0029-5515/33/7/I08

[14] A.N. Chudnovskiy, Yu.V. Gvozdkov, N.V. Ivanov, A.M. Kakurin, A.A. Medvedev, I.I. Orlovskiy, Yu.D. Pavlov, V.V. Piterskiy, V.D. Pustovitov, M.B. Safonova. Nucl. Fusion, **43**, 681 (2003). DOI: 10.1088/0029-5515/43/8/307

[15] R.J. La Haye, R. Fitzpatrick, T.C. Hender, A.W. Morris, J.T. Scoville, T.N. Todd. Phys. Fluids B, **4**, 2098 (1992). DOI: 10.1063/1.860017

[16] N.V. Ivanov, A.M. Kakurin. VANT. Ser. Termoyadernyi sintez, **1**, 64 (2012) (in Russian). http://vant.iterru.ru/vant_2012_1/6.pdf

[17] P.V. Savrukhin. Plasma Physics Reports, **27** (9), 727 (2001). DOI: 10.1134/1.1401935

[18] Yu.V. Petrov, M.I. Patrov, V.I. Varfolomeev, V.K. Gusev, E.A. Lamzin, N.V. Sakharov, S.E. Sychevsky. Fizika Plazmy, **36** (6), 492 (2010).

[19] P.V. Savrukhin. Plasma Physics Reports, **26**, 633 (2000). DOI: 10.1134/1.1306992

[20] E.A. Shestakov. *Upravlenie puchkami uskorennyh elektronov i MGD vozmushcheniyami s pomoshch'yu SVCH nagreva i rezonansnyh magnitnyh polej v plazme tokamaka T-10.* (Diss. M., 2019) (in Russian)

[21] E.A. Shestakov, P.V. Savrukhin, M.I. Ershova. J. Phys.: Conf. Ser., **1094**, 012005 (2018). DOI: 10.1088/1742-6596/1094/1/012005

[22] P.V. Savrukhin, E.A. Shestakov. Phys. Plasmas, **26**, 092505 (2019). DOI: 10.1063/1.5102112

Translated by A.Akhtayamov